Chapter 14
Effect of Time-Periodic Boundary Temperature Modulations on the Onset of Convection in a Maxwell Fluid–Nanofluid Saturated Porous Layer

Jawali C. Umavathi, Kuppalapalle Vajravelu, Prashant G. Metri and Sergei Silvestrov

Abstract The linear stability of Maxwell fluid–nanofluid flow in a saturated porous layer is examined theoretically when the walls of the porous layers are subjected to time-periodic temperature modulations. A modified Darcy–Maxwell model is used to describe the fluid motion, and the nanofluid model used includes the effects of the Brownian motion. The thermal conductivity and viscosity are considered to be dependent on the nanoparticle volume fraction. A perturbation method based on a small amplitude of an applied temperature field is used to compute the critical value of the Rayleigh number and the wave number. The stability of the system characterized by a critical Rayleigh number is calculated as a function of the relaxation parameter, the concentration Rayleigh number, the porosity parameter, the Lewis number, the heat capacity ratio, the Vadász number, the viscosity parameter, the conductivity variation parameter, and the frequency of modulation. Three types of temperature modulations are considered, and the effects of all three types of modulations are found to destabilize the system as compared to the unmodulated system.

J.C. Umavathi (✉)
Department of Mathematics, Gulbarga University, Gulbarga, Karnataka, India
e-mail: drumavathi@rediffmail.com

J.C. Umavathi
Department of Engineering, University of Sannio, Benevento, Italy

K. Vajravelu
Department of Mathematics, University of Central Florida, Orlando, FL 32816, USA
e-mail: kuppalapalle.vajravelu@ucf.edu

K. Vajravelu
Department of Mechanical, Material and Aerospace Engineering, University of Central Florida, Orlando, FL 32816, USA

P.G. Metri · S. Silvestrov
Division of Applied Mathematics, The School of Education, Culture and Communication, Mälardalen University, Box 883, 721 23 Västerås, Sweden
e-mail: prashant.g.metri@mdh.se

S. Silvestrov
e-mail: sergei.silvestrov@mdh.se

S. Silvestrov and M. Rančić (eds.), *Engineering Mathematics I*,
Springer Proceedings in Mathematics & Statistics 178,
DOI 10.1007/978-3-319-42082-0_14

Keywords Thermal modulation · Nanofluid · Galerkin method · Stability analysis

14.1 Introduction

Heat transfer enhancement in the base flow of fluid dispersion of nanoscale particles was reported by Masuda et al. [16]. The presence of nanoparticles in the fluid significantly increases the effective thermal conductivity of the mixture. The term nanofluid was coined by Choi [5] to refer to a fluid containing a dispersion of nanoparticles. These enhanced properties and behavior imply an enormous potential of nanofluids for device miniaturization and process intensification which could have impacts on many industrial sectors including chemical processing, transportation, electronics, medicine, energy, and the environment (see for details Chen et al. [4]). Several attempts were made to explain abnormal increases in the thermal conductivity and viscosity of nanofluids (Buongiorno [3], Vadász [34, 35]). However, a satisfactory explanation has yet to be found as emphasized by Eastman et al. [7] in their recent comprehensive review of the nanofluid literature. On the other hand, Buongiorno [3] focused on heat transfer enhancement of nanofluids in convective situations. He focused on the further heat transfer enhancement observed in convective situations: Buongiorno noted that the observation of convective heat transfer enhancement by several researchers could be due to the dispersion of the suspended nanoparticles, but he argued that this effect is too small to explain the observed enhancement. Also, Buongiorno noted that the absolute velocity of a nanoparticle could be viewed as the sum of the base fluid velocity and a relative velocity (that he called the slip velocity). He considered, in turn, seven slip mechanisms: inertia, Brownian diffusion, thermophoresis, diffusiophoresis, Magnus effect, fluid drainage, and gravity settling. After examining each of these effects, he concluded that in the absence of turbulence, the effects of the Brownian diffusion and the thermophoresis are important. Based on these two effects, Buongiorno formulated the conservation equations.

The Bénard problem (the onset of convection in a horizontal layer uniformly heated from below) for a nanofluid was studied by Tzou [32] on the basis of the transport equations of Buongiorno [3]. The corresponding problem for flow in a porous medium (the Horton–Rogers–Lapwood problem) was studied by Nield and Kuznetsov [21] using the Darcy model.

An alternative approach is to ignore special phenomena such as Brownian motion and thermophoresis but instead examine the effect of the variation of thermal conductivity and viscosity with the nanofluid particle fraction, using expressions used in the theory of mixtures. This approach was employed by Tiwari and Das [31] to study the cross-diffusion effects. It is assumed that the nanofluid is diluted so that the nanofluid volume fraction is small compared with unity. Then they assumed that the volume fraction is a linear function of the vertical coordinate. The vertical heterogeneity (especially the case of horizontal layers) was studied by McKibbin and O'Sullivan [18] and Leong and Lai [13]; and horizontal heterogeneity was studied by Nield [19], and Gounat and Caltagirone [10]. More general aspects of conductivity heterogeneity were discussed by Braester and Vadász [2], and Rees and Riley [23]. Simmons et al. [28] have pointed out that in many heterogeneous geological systems, hydraulic properties such as the hydraulic conductivity of the system under consideration can vary by many orders of magnitude and sometimes rapidly over small spatial scales. They also pointed out that the onset of instability is controlled by very local conditions in the vicinity of the evolving boundary layer and not by the global layer properties or indeed some average property of that macroscopic layer. They also pointed out that any averaging process would remove the very structural controls and physics that are expected to be important in controlling the onset, growth, and/or decay of instabilities in a highly heterogeneous system for the general case involving both vertical heterogeneity and horizontal heterogeneity. For this complicated situation no exact analytical solution can be expected to exist, but it is reasonable to seek an approximate analytical solution, based on the expectation that for weak heterogeneity, the solution would not differ dramatically from the solution for the homogeneous case. Following this approach, an extension of the Galerkin approximate method has been widely employed (see, for example, Finlayson [9]). In the context of the onset of convection, the commonly used Galerkin method involves trial functions of the vertical coordinate only. Thus, to a first approximation, the thermal conductivity and the viscosity can be taken as weak functions of the vertical coordinate. This means that we can treat the problem as one involving a weakly heterogeneous porous medium (Nield [20]).

Many working fluids of practical interest are viscoelastic rather than Newtonian. For this reason, current interest in this area is concerned with studies of the various viscoelastic models such as Maxwell fluids (Sokolov and Tanner [29]), Oldroyd type models (Khayat [12], Siddheshwar et al. [27]), Rivlin–Ericksen fluids (Siddheshwar and Srikrishna [26]), and Walters-B liquids (El-Sayed [8]). Analogous studies on viscoelastic fluid convection in porous media are those by Shekar and Jayalatha [24], Tan and Masuoka [30], and Shivakumara et al. [25].

Recently, Wang and Tan [36] have made a stability analysis of double diffusive convection of Maxwell fluid in a porous medium. It is worthwhile to point out that the first viscoelastic rate type model, which is still used widely, is due to Maxwell [17]. While Maxwell did not develop this model for polymeric liquids, he recognized that such fluid has a means for storing energy characterizing its viscous nature. Recently, Malashetty et al. [15] have studied double diffusive convection in a viscoelastic fluid saturated porous layer using the Oldroyd model. Very recently, Awad et al. [1] used the Darcy–Brinkman–Maxwell model to study linear stability analysis of a Maxwell fluid with cross-diffusion and double-diffusive convection.

Nonetheless, the studies related to the effects of thermal modulation on the onset of convection in a viscoelastic fluid-saturated porous medium have not received much attention. Chung Liu [6] has examined the stability of a horizontally extended second-grade fluid layer heated from below subject to temperature modulation at walls.

Motivated by the above studies, in the present paper, we study the effect of thermal modulation on the onset of convection in a Maxwell fluid and nanofluid saturated porous medium. The boundary temperature modulation alters the basic temperature distribution from linear to nonlinear which helps in effective control of convective instability. The difficulty in dealing with such instability problems is that one has to solve time-dependent stability equations with variable coefficients, and to our knowledge no work has been initiated for such fluids in this direction. The resulting eigenvalue problem is solved by a perturbation technique with amplitude of the temperature modulation as a perturbation parameter. In particular, it is shown that the onset of convection can be advanced by a proper tuning of the frequency of the boundary temperature modulation.

14.2 Mathematical Formulation

We consider an infinite horizontal porous layer saturated with a nanofluid, confined between the planes $z^* = 0$ and $z^* = H$, with the vertically downward gravity force acting on it. A Cartesian frame of reference is chosen with the origin in the lower boundary and the z-axis vertically upwards. The Boussinesq approximation, which states that the variation in density is negligible everywhere in the conservation except in the buoyancy term, is assumed to hold. The conservation equations take the form

$$\nabla^* \cdot v_D^* = 0. \tag{14.1}$$

Here v_D^* is the nanofluid Darcy velocity and $v_D^* = (u^*, v^*, w^*)$.

The conservation equation for the nanoparticles, in the absence of thermophoresis and chemical reactions, takes the form

$$\frac{\partial \phi^*}{\partial t^*} + \frac{1}{\varepsilon} v_D^* \cdot \nabla \phi^* = \nabla^* \cdot [D_B \nabla^* \phi^*], \tag{14.2}$$

where ϕ^* is the nanoparticle volume fraction, ε is the porosity, and D_B is the Brownian diffusion coefficient. We use the Darcy model for a porous medium. Hence, the momentum equation can be written as

$$\left(1 + \tilde{\lambda} \frac{\partial}{\partial t^*}\right) \frac{\rho}{\varepsilon} \frac{\partial v_D^*}{\partial t^*} = \left(1 + \tilde{\lambda} \frac{\partial}{\partial t^*}\right) (- \nabla^* p^* + \rho g) - \frac{\mu_{eff}}{K} v_D^*. \tag{14.3}$$

Here ρ is the overall density of the nanofluid, which we assume to be given by

$$\rho = \phi^* \rho_p + (1 - \phi^*) \rho_0 [1 - \beta_T (T^* - T_0^*)], \tag{14.4}$$

where ρ_p is the particle density, ρ_0 is a reference density for the fluid, and β_T is the thermal volumetric expansion. The thermal energy equation for a nanofluid can be written as

$$(\rho c)_m \frac{\partial T^*}{\partial t^*} + (\rho c)_f v_D^* \cdot \nabla^* T^* = k_m \nabla^{*2} T^* + \varepsilon (\rho c)_p [D_B \nabla^* \phi^* \cdot \nabla T^*]. \tag{14.5}$$

The conservation of nanoparticle mass requires that

$$\frac{\partial \phi^*}{\partial t^*} + \frac{1}{\varepsilon} v_D^* \cdot \nabla^* \phi^* = D_p \nabla^{*2} \phi^*. \tag{14.6}$$

Here c is the fluid specific heat (at constant pressure), k_m is the overall thermal conductivity of the porous medium saturated by the nanofluid, and c_p is the nanoparticle specific heat of the material constituting the nanoparticles (following Nield and Kuznetsov [22]). Thus,

$$k_m = \varepsilon k_{eff} + (1-\varepsilon) k_s, \tag{14.7}$$

where k_{eff} is the effective conductivity of the nanofluid (fluid plus nanoparticles) and k_s is the conductivity of the solid material forming the matrix of the porous medium.

We now introduce the viscosity and the conductivity dependence on nanoparticle fraction. Following Tiwari and Das [31], we adopt the formulas, based on a theory of mixtures,

$$\frac{\mu_{eff}}{\mu_f} = \frac{1}{(1-\phi^*)^{2.5}}, \tag{14.8}$$

$$\frac{k_{eff}}{k_f} = \frac{(k_p + 2k_f) - 2\phi^*(k_f - k_p)}{(k_p + 2k_f) + \phi^*(k_f - k_p)}. \tag{14.9}$$

Here k_f and k_p are the thermal conductivities of the fluid and the nanoparticles, respectively. In the case where ϕ^* is small compared with unity, we can approximate these formulas by

$$\frac{\mu_{eff}}{\mu_f} = 1 + 2.5\phi^*, \tag{14.10}$$

$$\frac{k_{eff}}{k_f} = \frac{(k_p + 2k_f) - 2\phi^*(k_f - k_p)}{(k_p + 2k_f) + \phi^*(k_f - k_p)} = 1 + 3\phi^* \frac{(k_p - k_f)}{(k_p + 2k_f)}. \tag{14.11}$$

We assume that the volumetric fractions of the nanoparticles are constant on the boundaries. Thus, the boundary conditions are

$$w^* = 0, \quad \phi^* = \phi_0^* \quad \text{at} \quad z^* = 0, \tag{14.12}$$

$$w^* = 0, \quad \phi^* = \phi_1^* \quad \text{at} \quad z^* = H. \tag{14.13}$$

For thermal modulation, the external driving force is modulated harmonically in time by varying the temperature of the lower and upper horizontal boundary. Accordingly, we take

$$T(z,t) = T_0 + \frac{\triangle T}{2}[1 + \varepsilon_1 cos(\Omega t)] \quad \text{at} \quad z^* = 0, \tag{14.14}$$

$$T(z,t) = T_0 - \frac{\triangle T}{2}[1 - \varepsilon_1 cos(\Omega t + \phi)] \quad \text{at} \quad z^* = H, \tag{14.15}$$

where ε_1 represents a small amplitude of modulation (which is used as a perturbation parameter to solve the problem), Ω the frequency of modulation, and ϕ the phase angle. We consider three types of modulation, viz.,
Case (a): Symmetric (in phase, $\phi = 0$),
Case (b): Asymmetric (out of phase, $\phi = \pi$), and
Case (c): Only lower wall temperature is modulated while the upper one is held at constant temperature ($\phi = -i\infty$).

14.3 Basic State Problem

The basic state of the fluid is quiescent and is given by

$$\rho_b \vec{g} + \nabla p_b = 0, \tag{14.16}$$

$$(\rho c)_m \frac{\partial T_b^*}{\partial t^*} = k_m \nabla^2 T^*, \tag{14.17}$$

$$\frac{d^2 \phi_b^*}{dz^2} = 0. \tag{14.18}$$

The solution of (14.17) satisfying the thermal conditions as given in (14.14) and (14.15) is $T_b = T_1(z) + \varepsilon_t T_2(z,t)$ where

$$T_1(z) = T_R + \frac{\triangle T}{2}\left(1 - \frac{2z}{H}\right), \tag{14.19}$$

$$T_2(z,t) = Re[\{b(\lambda)e^{\frac{\lambda z}{H}} + b(-\lambda)e^{\frac{-\lambda z}{H}}\}e^{-i\omega t}], \tag{14.20}$$

with

$$\lambda = (1-i)\left(\frac{(\rho c)_m \omega H^2}{2k_m}\right), \quad b(\lambda) = \frac{\triangle T}{2}\left(\frac{e^{-i\phi} - e^{-\lambda}}{e^{\lambda} - e^{-\lambda}}\right), \tag{14.21}$$

and Re stands for real part. We do not record the expressions of p_b and ρ_b as these are not explicitly required in the remaining part of the paper.

14.4 Linear Stability Analysis

Let the basic state be distributed by an infinitesimal perturbation. We now have,

$$v = v^{'}, \quad p = p_b + p^{'}, \quad T = T_b + T^{'}, \quad \phi = \phi_b + \phi^{'}, \tag{14.22}$$

where a prime indicates that the quantities are infinitesimal perturbations. Substituting (14.22) into (14.1)–(14.7) and linearizing by neglecting products of primed quantities, we have,

$$(1 + \lambda_1 s)(\nabla p - RT\widehat{e_z} + Rn\phi\widehat{e_z} + \gamma_a s v) + \tilde{\mu} v = 0, \tag{14.23}$$

$$\frac{\partial T^{'}}{\partial t} + w^{'}\frac{\partial T_b}{\partial z} = \tilde{k}\frac{\partial^2 T}{\partial z^2} + \frac{N_B}{Le}\left(\frac{\partial T_b}{\partial z} + \frac{\partial T^{'}}{\partial z} + \frac{\partial \phi^{'}}{\partial z}\frac{\partial T_b}{\partial z}\right), \tag{14.24}$$

$$\frac{1}{\sigma}\frac{\partial \phi^{'}}{\partial t} + \frac{1}{\varepsilon}w^{'} = \frac{1}{Le}\nabla^2 \phi^{'}, \tag{14.25}$$

$$w^{'} = 0, \ T^{'} = 0, \ \phi^{'} = 0 \quad \text{at} \quad z = 0, 1. \tag{14.26}$$

We introduce the following transformations:

$$(x, y, z) = \frac{(x^*, y^*, z^*)}{H}, \ t = \frac{t^*\alpha_m}{\sigma H^2}, \ (u, v, w) = \frac{(u^*, v^*, w^*)H}{\alpha_m}, \ p = \frac{p^* K}{\mu_f \alpha_m},$$
$$\phi = \frac{\phi^* - \phi_0^*}{\phi_1^* - \phi_0^*}, \ T = \frac{T^* - T_c^*}{T_h^* - T_c^*}, \ \omega = \frac{\sigma \Omega H^2}{\alpha_m}, \ s = \frac{\partial}{\partial t},$$

with

$$\alpha_m = \frac{k_m}{(\rho c_p)_f}, \ \sigma = \frac{(\sigma c_p)_m}{(\rho c_p)_f}, \ \tilde{\mu} = \frac{\mu_{eff}}{\mu_f}, \ \tilde{k_p} = \frac{k_p}{k_f}, \ \tilde{k_s} = \frac{k_s}{k_f}, \ \tilde{k} = \frac{k_m}{k_s}.$$

The dimensionless parameters that appear are these:

- $Pr = \frac{\mu_f}{\rho \alpha_m}$ - the Prandtl number,
- $Da = \frac{K}{H^2}$ - the Darcy number,
- $Va = \frac{\varepsilon^2 Pr}{Da}$ - the Vadász number,
- $\lambda_1 = \frac{\tilde{\lambda}\alpha_m}{\sigma H^2}$ - the relaxation parameter (also known as the Deborah number),
- $\gamma_a = \frac{\varepsilon}{\sigma Va}$ - the acceleration coefficient,
- $Le = \frac{\alpha_m}{D_m}$ - the nanofluid Lewis number,
- $R = \frac{R_0 g K (1-\phi_0^*)\beta_T \triangle T^* H}{\mu_f \alpha_m}$ - the nanoparticle Rayleigh number, and
- $N_B = \frac{(\rho c_p)_p}{(\rho c)_f}(\phi_1^* - \phi_0^*)$ - modified particle-density increment.

In deriving (14.23), the term proportional to the product of ϕ and T (Oberbeck–Boussinesq approximation) is neglected. This assumption is likely to be valid in the case of small temperature gradients in a dilute suspension of nanoparticles: For regular fluid the parameters Rn and N_B are zeros.

We eliminate pressure by operating on (14.23) with $\widehat{e_z}$ curl curl and using the identity *curl curl* $\equiv$ *grad div* $- \nabla^2$ results in

$$[(1+\lambda_1 s)s\gamma_a + \tilde{\mu}]\,\nabla^2 w' = (1+\lambda_1 s)[R\,\nabla_H^2 - Rn\,\nabla_H^2\,\phi']. \tag{14.27}$$

Here ∇_H^2 is the two-dimensional Laplacian operator on the horizontal plane. By combining the (14.24)–(14.26), we obtain the equations for the vertical component of velocity w in the form (dropping prime)

$$\begin{aligned}\left[\frac{\partial}{\partial t} - \nabla^2\gamma\right]\left[\frac{1}{\sigma}\frac{\partial}{\partial t} - \frac{\nabla^2}{Le}\right][\nu + s\gamma_a(1+\lambda_1 s)]\,\nabla^2 w - \\ - \frac{(1+\lambda_1 s)Rn}{\varepsilon}\left[\frac{\partial}{\partial t} - \nabla^2\gamma\right]\nabla_1^2 w + \\ +(1+\lambda_1 s)R\frac{\partial T_b}{\partial z}\left[\frac{1}{\sigma}\frac{\partial}{\partial t} - \frac{\nabla^2}{Le}\right]\nabla_1^2 w = 0,\end{aligned} \tag{14.28}$$

where, $\nu = 1 + 1.25(\phi_1^* + \phi_0^*)$, and $\eta = \varepsilon + (1-\varepsilon)\tilde{k_s} + \frac{3(\phi_1^*+\phi_0^*)\varepsilon}{2}\left(\frac{\tilde{k_p}-1}{\tilde{k_p}+2}\right)$.

It is worth noting that the factor ν comes from the mean value of $\tilde{\mu}(z)$ over the range [0, 1], and the factor η is the mean value of $\tilde{k}(z)$ over the same range. That means that when evaluating the critical Rayleigh number, it is a good approximation to base that number on the mean values of the viscosity and conductivity based in turn on the basic solution for the nanofluid fraction (following Nield and Kuznetsov [22]).

The boundary condition (14.26) is applied to (14.27) resulting in the following boundary condition for w:

$$w = \frac{d^2 w}{dz^2} = 0 \quad \text{at} \quad z = 0, 1. \tag{14.29}$$

Using (14.19), the dimensionless temperature gradient appearing in (14.24) may be written as

$$\frac{\partial T_b}{\partial z} = -1 + \varepsilon f, \tag{14.30}$$

where

$$f = Re\left[A(\lambda)e^{\lambda z} + A(-\lambda)e^{-\lambda z}e^{-i\omega}t\right], \text{ for} \tag{14.31}$$

$$A(\lambda) = \frac{\lambda}{2}\left(\frac{e^{-i\varphi} - e^{-\lambda}}{e^{\lambda} - e^{-\lambda}}\right), \text{ and } \lambda = (1-i)\left(\frac{\sigma\omega}{2}\right)^{\frac{1}{2}}.$$

14.5 Method of Solution

We seek the eigenfunctions w and eigenvalues Ra of (14.28) for the basic temperature gradient given by (14.30) that departs from the linear profile $\frac{\partial T_b}{\partial z} = -1$ by quantities of order ε_1. We therefore assume the solution of (14.28) is in the form

$$(w, R) = (w_0, R_0) + \varepsilon_1(w_1, R_1) + \varepsilon_1^2(w_2, R_2) + \dots \,. \tag{14.32}$$

Substituting (14.32) into (14.28) and equating the coefficients of various powers of ε_t on either side of the resulting equation, we obtain the following system of equations up to the order of ε_t^2:

$$Lw_0 = 0, \tag{14.33}$$

$$Lw_1 = (1 + \lambda_1 s)\left[\left(\frac{R_0\omega G}{\sigma}\,\nabla_1^2 + \frac{R_0 f}{Le}\right)\nabla_1^2 - \frac{R_1}{Le}\,\nabla^2\,\nabla_1^2\right] w_0, \tag{14.34}$$

$$\begin{aligned} Lw_2 = (1 + \lambda_1 s)\left[R_0\left(\frac{\omega G}{\sigma} + \frac{f}{Le}\nabla^2\right) - \frac{R_1}{Le}\nabla^2\right]\nabla_1^2\, w_1 + \\ +(1 + \lambda_1 s)R_1\left(\frac{\omega G}{\sigma} + \frac{f}{Le}\,\nabla^2 + \frac{R_2}{Le}\nabla^2\right)\nabla_1^2\, w_0, \end{aligned} \tag{14.35}$$

where

$$\begin{aligned} L = \left(1 + \lambda\frac{\partial}{\partial t}\right)\left(\frac{\partial}{\partial t} - \nabla^2\gamma\right)\left(\frac{1}{\sigma}\frac{\partial}{\partial t} - \frac{\nabla^2}{Le}\right)\left(\nu + \gamma_a\frac{\partial}{\partial t}\right)\nabla^2 - \\ -\frac{Rn}{\varepsilon}\left(\frac{\partial}{\partial t} - \nabla^2\gamma\right)\nabla_1^2 + \frac{R_0}{Le}\,\nabla^2\,\nabla_1^2, \end{aligned}$$

and w_0, w_1, w_2 are required to satisfy the boundary condition in (14.29).

We now assume the solutions for (14.33) are of the form $w_0 = w_0(z)exp[i(lx + my)]$ where $w_0(z) = w_0^n(z) = sin(n\pi z)$, $n = 1, 2, 3\dots$ and l, m are the wave numbers in the xy plane such that $l^2 + m^2 = \alpha^2$. The corresponding eigenvalues are given by

$$R_0 = \frac{(n^2\pi^2 + \alpha^2)^2\nu\gamma}{\alpha^2} - \frac{RnLe\gamma}{\varepsilon}. \tag{14.36}$$

For a fixed value of the wave number α, the least eigenvalue occurs at $n = 1$ and is given by

$$R_0 = \frac{(\pi^2 + \alpha^2)^2\nu\gamma}{\alpha^2} - \frac{RnLe\gamma}{\varepsilon}, \tag{14.37}$$

and R_{0c} assumes the minimum value

$$R_{0c} = 4\pi^2\nu\gamma - \frac{RnLe\gamma}{\varepsilon}. \tag{14.38}$$

These are the values reported by Horton and Rogers [11] in the absence of concentration Rayleigh number Rn.

The equation for w_1 then takes the form

$$Lw_1 = R_0\alpha^2(1-\lambda_1 i\omega)\left(\frac{\omega}{\sigma}G + \frac{(D^2-\alpha^2)f}{Le}\right)\sin\pi z, \tag{14.39}$$

where $D = \frac{d}{dz}$ and $G = I.P.[\{A(\lambda)e^{\lambda z}\} + \{A(-\lambda)e^{-\lambda z}\}e^{-i\omega t}]$. Thus,

$$D^2 f\sin\pi z = (\lambda^2-\pi^2)f\sin\pi z + 2\lambda\pi f'\cos\pi z \tag{14.40}$$

with $f' = R.P.[\{A(\lambda)e^{\lambda z}\} + \{A(-\lambda)e^{-\lambda z}\}e^{-i\omega t}]$.

Using (14.40), (14.39) becomes

$$Lw_1 = R_0\alpha^2(-1+\lambda_1 i\omega)\left(\frac{\omega}{\sigma}G\sin\pi z - L_1 f\sin\pi z + \frac{2\lambda\pi f'}{Le}\cos\pi z\right), \tag{14.41}$$

where $L_1 = \frac{i\omega+\pi^2+\alpha^2}{Le}$.

We solve (14.41) for w_1 by expanding the right hand side of it in Fourier series expansion and inverting the operator L for this we need the following Fourier series expansions

$$g_{nm}(\lambda) = 2\int_0^1 e^{\lambda z}\sin(m\pi z)\sin(n\pi z)dz = \frac{-4nm\pi^2\lambda[1+(-1)^{n+m+1}e^z]}{[\lambda^2+(n+m)^2\pi^2][\lambda^2+(n-m)^2\pi^2]}, \tag{14.42}$$

$$f_{nm}(\lambda) = 2\int_0^1 e^{\lambda z}\cos(m\pi z)\cos(n\pi z)dz = \frac{2\lambda[\lambda^2+(n+m)^2\pi^2][1+(-1)^{n+m+1}e^z]}{[\lambda^2+(n+m)^2\pi^2][\lambda^2+(n-m)^2\pi^2]}, \tag{14.43}$$

where

$$e^{\lambda z}\sin(m\pi z) = \sum_{n=1}^{\infty} g_{nm}(\lambda)\sin(n\pi z), \tag{14.44}$$

$$e^{\lambda z}\cos(m\pi z) = \sum_{n=1}^{\infty} f_{nm}(\lambda)\cos(n\pi z). \tag{14.45}$$

Now,

$$L(\omega, n) = A + i\omega B, \tag{14.46}$$

where

$$A = \left[\omega^2\gamma_a(n^2\pi^2+\alpha^2)^2\left(\frac{1}{Le}+\frac{\gamma}{\sigma}\right)(1+\lambda_1\nu)+\frac{\omega^2}{\sigma}(n^2\pi^2+\alpha^2)(\nu-\lambda_1\omega^2\gamma_a)+\right.$$
$$+(n^2\pi^2+\alpha^2)^3\frac{\gamma}{Le}(-\nu+\lambda_1\omega^2\gamma_a)+\frac{Rn}{\varepsilon}\alpha^2(\gamma(n^2\pi^2+\alpha^2)-\lambda_1\omega^2)+$$
$$\left.+\left(4\pi^2\nu\gamma-\frac{RnLe\gamma}{\varepsilon}\right)\frac{\alpha^2}{Le}(n^2\pi^2+\alpha^2)\right],$$

$$B = \left[(n^2\pi^2+\alpha^2)^2\left(\frac{1}{Le}+\frac{\gamma}{\sigma}\right)(\nu-\lambda_1\gamma_a\omega^2)+\frac{\omega^2}{\sigma}(n^2\pi^2+\alpha^2)(-\gamma_a-\lambda_1\nu)+\right.$$
$$+(n^2\pi^2+\alpha^2)^3\frac{\gamma}{Le}(\gamma_a+\lambda_1\nu)+\frac{Rn}{\varepsilon}\alpha^2(-1+\gamma\lambda_1(n^2\pi^2+\alpha^2))-$$
$$\left.-\left(4\pi^2\nu\gamma-\frac{RnLe\gamma}{\varepsilon}\right)\frac{\alpha^2\lambda_1}{Le}(n^2\pi^2+\alpha^2)\right].$$

It is easily seen that:

$$L\left[\sin(n\pi z)e^{-i\omega t}\right] = L(\omega, n)\sin(n\pi z)e^{i\omega t},$$

and

$$L\left[\cos(n\pi z)e^{-i\omega t}\right] = L(\omega, n)\cos(n\pi z)e^{i\omega t},$$

and (14.41) now becomes

$$Lw_1 = (-1+\lambda_1 i\omega)\alpha^2 R_0\left[\frac{\omega}{\sigma}I.P.\sum_{n=1}^{\infty}A_n(\lambda)\sin n\pi z e^{i\omega t}-\right. \tag{14.47}$$
$$\left.-L_1 R.P.\sum_{n=1}^{\infty}A_n(\lambda)\sin n\pi z e^{i\omega t}+\frac{2\lambda\pi}{Le}R.P.\sum_{n=1}^{\infty}B_n(\lambda)\cos n\pi z e^{i\omega t}\right],$$

$$Lw_1 = (-1+\lambda_1 i\omega)\alpha^2 R_0\left[\frac{\omega}{\sigma}I.P.\sum_{n=1}^{\infty}\frac{A_n(\lambda)}{L(\omega, n)}\sin n\pi z e^{i\omega t}-\right. \tag{14.48}$$
$$-L_1 R.P.\sum_{n=1}^{\infty}\frac{A_n(\lambda)}{L(\omega, n)}\sin n\pi z e^{i\omega t}+$$

$$+\frac{2\lambda\pi}{Le}R.P.\sum_{n=1}^{\infty}\frac{B_n(\lambda)}{L(\omega,n)}\cos n\pi z e^{i\omega t}\Bigg],$$

where $A_n = A(\lambda)g_{n1}(\lambda) + A(-\lambda)g_{n1}(-\lambda)$, and $B_n = A(\lambda)f_{n1}(\lambda) + A(-\lambda)$ $f_{n1}(-\lambda)$.

To simplify (14.34) for w_2 we need

$$Lw_2 = (1+\lambda_1 s)\left[R_0\left(\frac{\omega G}{\sigma}+\frac{\nabla^2 f}{Le}\right)\nabla_1^2 w_1 - R_2\frac{\nabla^2}{Le}\cdot\nabla_1^2 w_1\right]. \tag{14.49}$$

The equation for then can be written as

$$Lw_2 = (1-\lambda_1 i\omega)\left[R_0\left(\frac{\omega G}{\sigma}-L_n f\right)w_1+\frac{2DfDw_1}{Le}\right]-R_2\frac{\alpha^2}{Le}(\pi^2+\alpha^2), \tag{14.50}$$

where $L_n = \frac{i\omega+n^2\pi^2+\alpha^2}{Le}$.

We shall not require the solution of this equation but merely use it to determine R_2. The solvability condition requires that the time-independent part of the right hand side of (14.50) must be orthogonal to $\sin(\pi z)$. Multiplying equation (14.50) by $\sin(\pi z)$ and integrating between 0 and 1 we obtain

$$R_2 = \frac{2LeR_0(1-2i\lambda\omega)}{\nabla^2}\int_0^1\left(\overline{\frac{\nabla^2 f}{Le}\frac{\omega G}{\sigma}}\right)w_1\sin(\pi z)dz, \tag{14.51}$$

where an upper bar denotes the time average.

We have the Fourier series expansions

$$f\sin\pi z = R.P.\sum A_n(\lambda)\sin n\pi z e^{i\omega t}, \tag{14.52}$$

$$Df\sin\pi z = R.P.\sum \lambda C_n(\lambda) sin n\pi z e^{i\omega t},$$

where $C_n(\lambda) = A(\lambda)g_{n1}(\lambda) - A(-\lambda)g_{n1}(-\lambda)$.

Using (14.52) in (14.51) we obtain

$$R_2 = \frac{LeR_0^2\alpha^2}{2(\pi^2+\alpha^2)}\cdot \tag{14.53}$$

$$\left[\left(-\frac{\omega^2}{\sigma^2}-\overline{L_n}L_1\right)R.P.\sum\frac{|A_n|^2}{|L(\omega,n)|^2}L^*(\omega,n)(1-2i\lambda_1\omega)(-1+i\lambda_1\omega)+\right]$$

$$+\left[\frac{4n\pi^2\lambda_1}{Le^2}R.P.\sum\overline{\lambda_1 C_n}\frac{B_n}{|L(\omega,n)|^2}L^*(\omega,n)(1-2i\lambda_1\omega)(-1+i\lambda_1\omega)\right],$$

where $L^*(\omega, n)$ is the complex conjugate of $L(\omega, n)$, and

$$| A_n(\lambda) |^2 = \frac{16n^2\pi^4\omega^2}{(\omega^2 + (n+1)^4\pi^4)(\omega^2 + (n-1)^4\pi^4)}.$$

The critical value of R_2, denoted by R_{2c}, is obtained at the wave number given by equation $\alpha_c = \pi$ for the following three different cases:

1. When the oscillating temperature field is symmetric so that the wall temperatures are modulated in phase (with $\phi = 0$).
2. When the wall temperature field is antisymmetric corresponding to out-of-phase modulation (with $\phi = \pi$).
3. When only the temperature of the bottom wall is modulated, the upper wall being held at a constant temperature (with $\phi = -i\infty$).

14.6 Results and Discussion

The effect of thermal modulation on the onset of convection in a layer of Maxwell fluid and nanofluid saturated porous medium is investigated using linear stability analysis. A perturbation technique with amplitude of the modulating temperature as a perturbation parameter is used to find the critical thermal Rayleigh number as a function of frequency of the modulation, relaxation parameter, concentration Rayleigh number, porosity parameter, Lewis number, heat capacity ratio, Vadász number, conductivity, and viscosity variation parameters. The sign of R_{2c} characterizes the stabilizing or destabilizing effects of modulation. A positive R_{2c} indicates that the modulation effect is to stabilize the flow: while a negative R_{2c} indicates the effect is to destabilize, compared to the system in which modulation is absent. We present below the results for three different wall temperature oscillating mechanisms: They are, symmetric, asymmetric, and lower wall temperature modulation only.

In Figs. 14.1, 14.2, 14.3, 14.4, 14.5, 14.6, 14.7 and 14.8, the variations of critical Rayleigh number R_{2c} with frequency ω for different governing parameters are presented for the case of symmetric temperature modulation. It can be seen from these figures that for small frequencies the critical Rayleigh number R_{2c} is negative indicating the destabilized flow. For moderate and high frequencies, the critical Rayleigh number R_{2c} is positive indicating that the effect of symmetric modulation is to stabilize the system. It can also be seen that as R_{2c} decreases to its minimum value (thus producing maximum destabilization), and then increases to its maximum stabilizing value, and finally decreases to zero as the frequency increases from zero to infinity. That is, in the presence of thermal modulation, convection occurs at lower values of the Rayleigh number compared to the unmodulated system.

Figure 14.1 shows the effect of the relaxation parameter λ_1 on the critical Rayleigh number R_{2c} for fixing the other governing parameters in the case of symmetric modulation. It is seen that an increase in the value of the relaxation parameter increases the

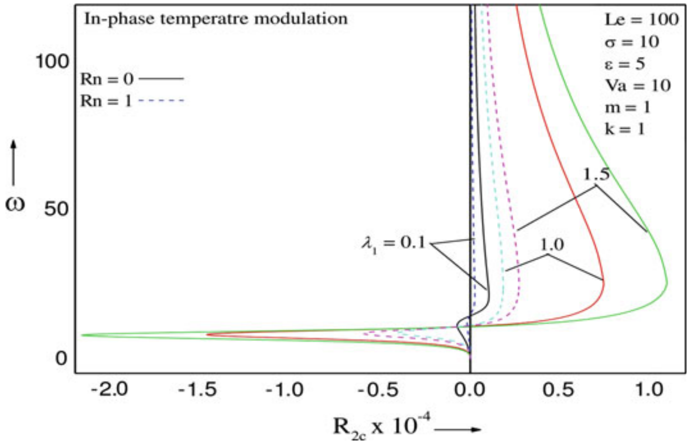

Fig. 14.1 Variation of R_{2c} with ω for different values of λ_1 and Rn

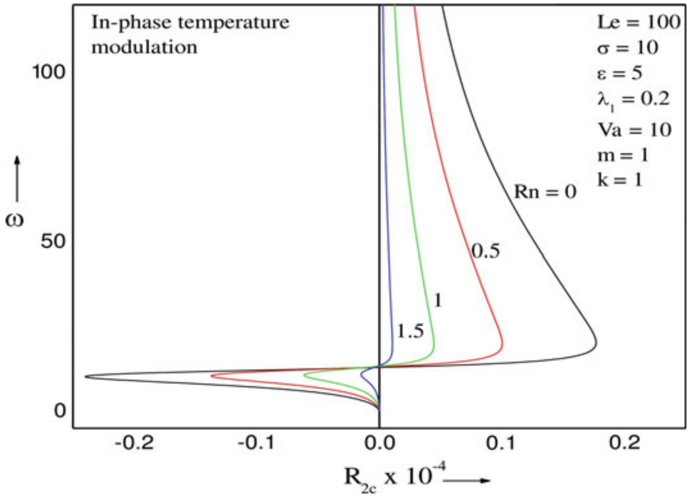

Fig. 14.2 Variation of R_{2c} with ω for different values of Rn

magnitude of R_{2c}. At small frequencies, R_{2c} increases negatively, while R_{2c} increases positively with the relaxation parameter at moderate and high frequencies for both regular and nanofluids. Hence the effect of the relaxation parameter is to destabilize the system for small frequencies while its effect is to stabilize the system for moderate and high frequencies. This agrees well with the results obtained by Malashetty and Begum [14] for a clear fluid. Figure 14.1 also indicates that the peak negative value of R_{2c} increases with an increase in the value of λ_1 which is the result obtained by Shivakumara et al. [25] for a viscoelastic fluid.

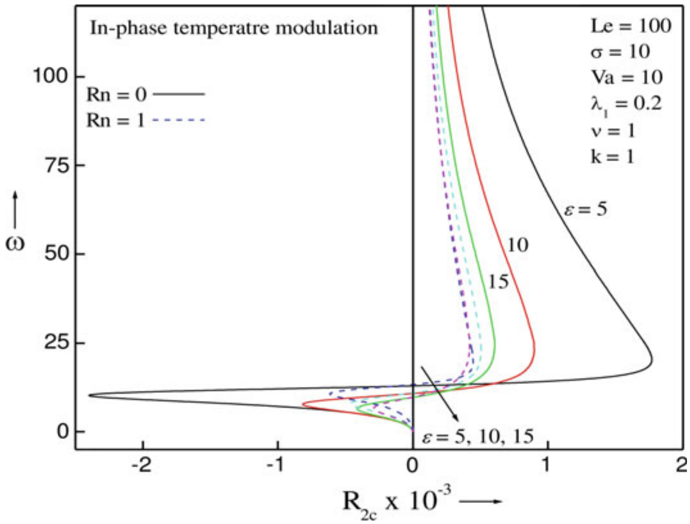

Fig. 14.3 Variation of R_{2c} with ω for different values of ε and Le

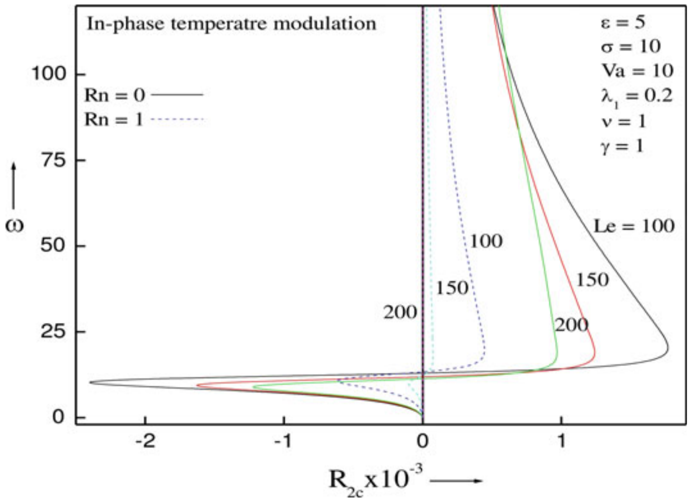

Fig. 14.4 Variation of R_{2c} with ω for different values of Rn and Le

Figure 14.2 shows the variation of R_{2c} with ω for different values of the concentration Rayleigh number Rn : $Rn > 0$ indicates top heavy nanoparticles and $Rn < 0$ indicates bottom heavy nanoparticles. Here also it is observed that for small frequencies, R_{2c} is negative indicating that the symmetric modulation has destabilizing effect while for moderate and large values of frequencies its effect is stabilizing for both regular and nanofluids. This is similar to the observed results of Umavathi [33]. The effect of porosity parameter ε for symmetric modulation is shown in Fig. 14.3. It is

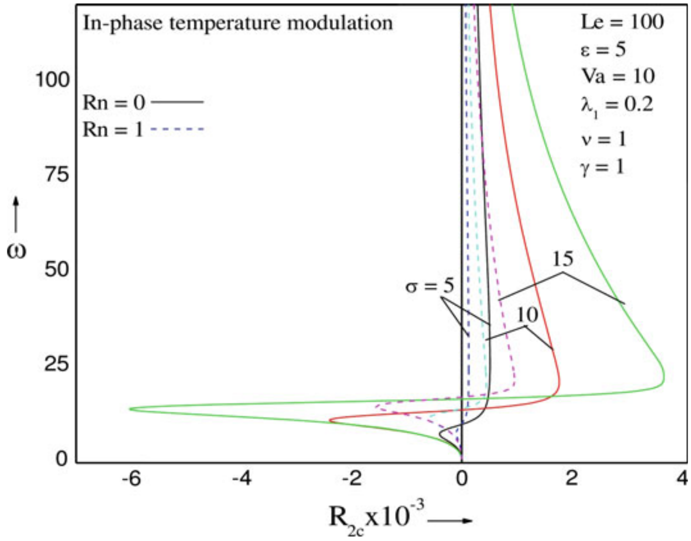

Fig. 14.5 Variation of R_{2c} with ω for different values of Rn and σ

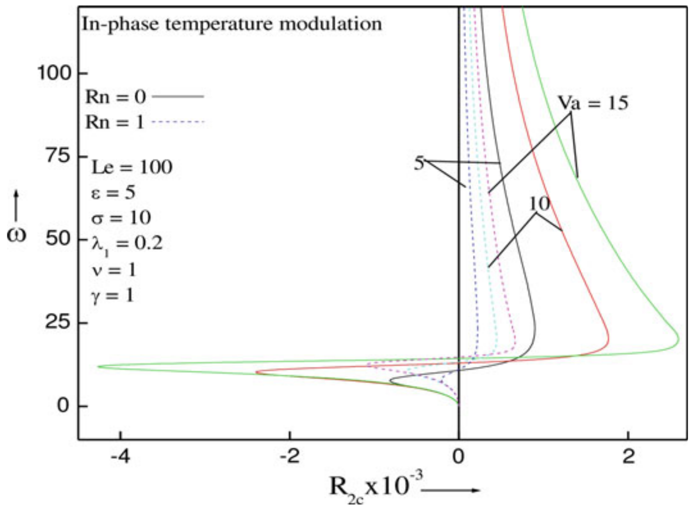

Fig. 14.6 Variation of R_{2c} with ω for different values of Rn and Vadász number Va

observed that as ε increases, the value of $| R_{2c} |$ becomes small indicating that the larger values of ε decrease the effect of modulation. Here also it is observed that as ω increases, R_{2c} increases to its maximum value initially and then starts decreasing with further increase in ω. When ω is very large, all the curves for different porosity ε coalesce and $| R_{2c} |$ approaches to zero. Figure 14.4 depicts the variation of R_{2c} with frequency ω for different values of Lewis number Le. An increase in the value of the

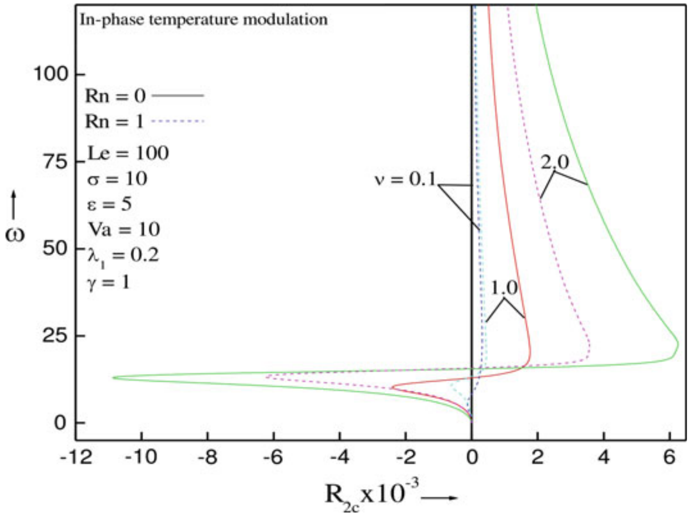

Fig. 14.7 Variation of R_{2c} with ω for different values of Rn and ν

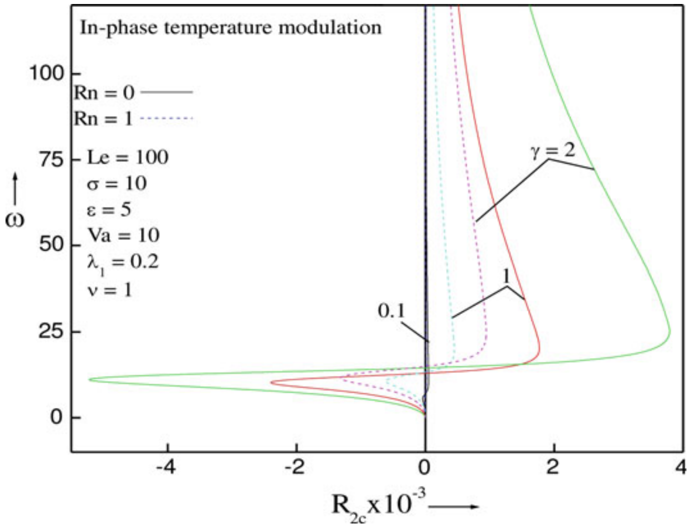

Fig. 14.8 Variation of R_{2c} with ω for different values of Rn and γ

Lewis number decreases the value of $| R_{2c} |$ indicating that the effect of increasing Le is to reduce the effect of thermal modulation for regular and nanofluids. As ω increases, $| R_{2c} |$ increases to its maximum value initially and then decreases with further increase in ω. For large, ω all the curves for different Lewis number coincide, and $| R_{2c} |$ approaches to zero for both regular and nanofluids. The effect of thermal capacity ratio σ and ω is shown in Fig. 14.5. As σ increases, $| R_{2c} |$ decreases for

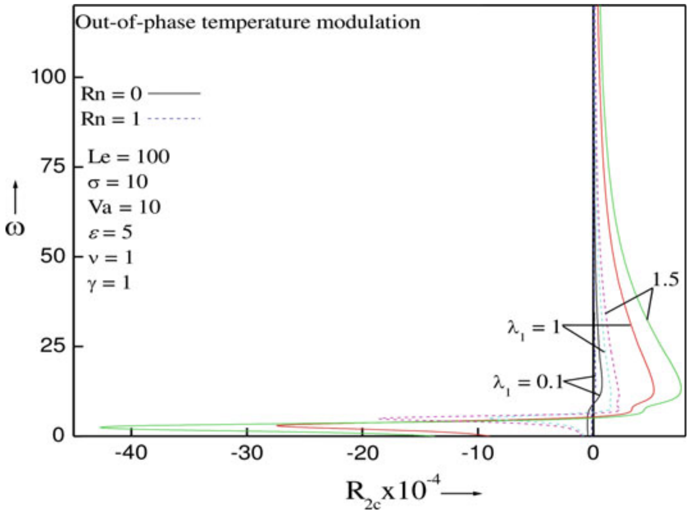

Fig. 14.9 Variation of R_{2c} with ω for different values of Rn and λ_1

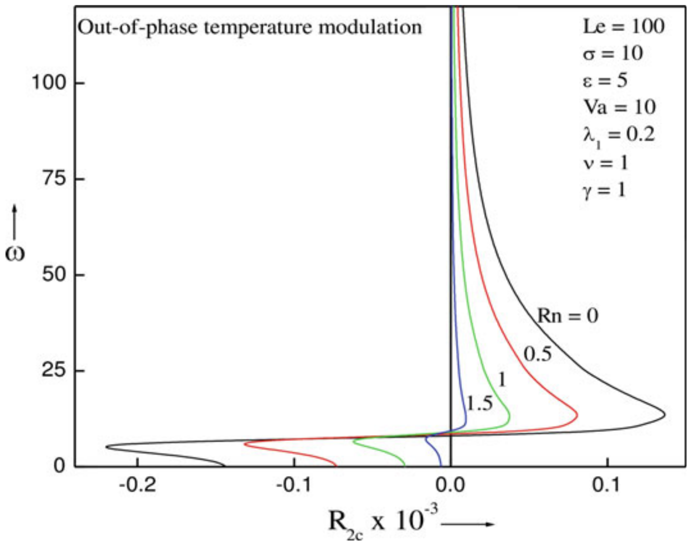

Fig. 14.10 Variation of R_{2c} with ω for different values of Rn

both regular and nanofluids. Here also $| R_{2c} |$ increases to its maximum value initially as ω increases and then starts decreasing with further increase in ω. The effect of Vadász number Va shows a similar nature as that of heat capacity ratio σ as seen in Fig. 14.6. The effects of viscosity variation parameter υ and conductivity variation parameter γ are shown in Figs. 14.7 and 14.8, respectively. As υ and γ increase, $| R_{2c} |$ decreases indicating that the viscosity and conductivity ratio stabilizes the

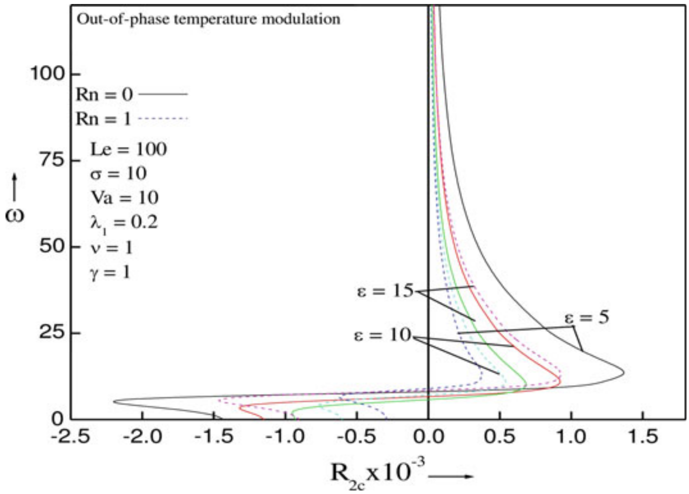

Fig. 14.11 Variation of R_{2c} with ω for different values of Rn and ε

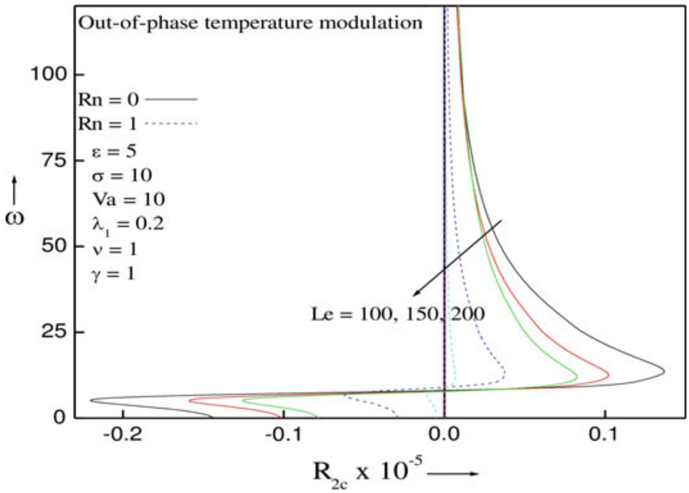

Fig. 14.12 Variation of R_{2c} with ω for different values of Rn and Le

system. As ω increases, $|\ R_{2c}\ |$ increases to its maximum value initially and then starts decreasing with further increase in ω.

The results obtained for the case of asymmetric modulation are presented in Figs. 14.9, 14.10, 14.11, 14.12, 14.13, 14.14, 14.15 and 14.16. All these figures show that for all parameters, small frequencies have destabilizing effects while for moderate and large values of the frequency, their effects are to stabilize the system. It is seen from Fig. 14.9 that an increase in the value of λ_1 increases the magnitude of R_{2c}. The effect of the concentration Rayleigh number Rn, porosity parameter ε, Lewis

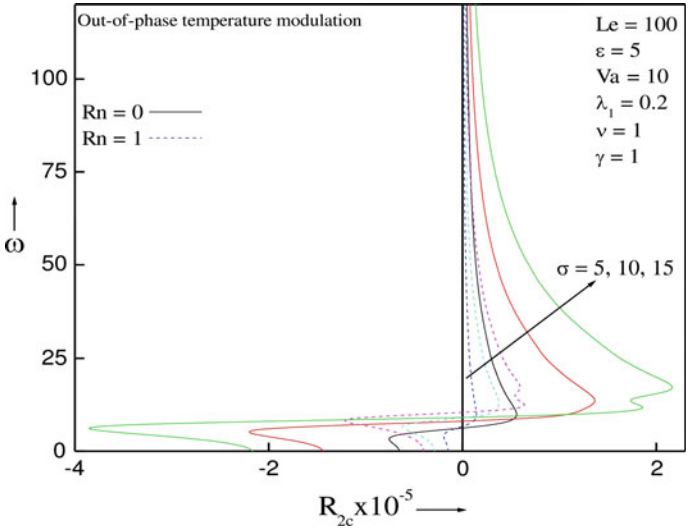

Fig. 14.13 Variation of R_{2c} with ω for different values of Rn and σ

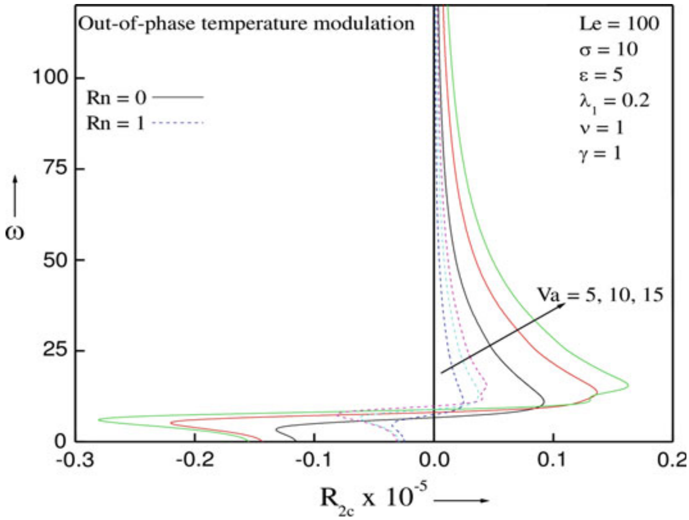

Fig. 14.14 Variation of R_{2c} with ω for different values of Rn and Va

number Le, thermal capacity ratio σ, Vadász number Va, viscosity and conductivity variation parameters υ and γ is the same as in the case of symmetric modulation, and hence a detailed explanation is not presented. The variation of all the governing parameters for the case of only lower wall temperature modulation produce similar effects as for asymmetric modulation and hence not shown pictorially.

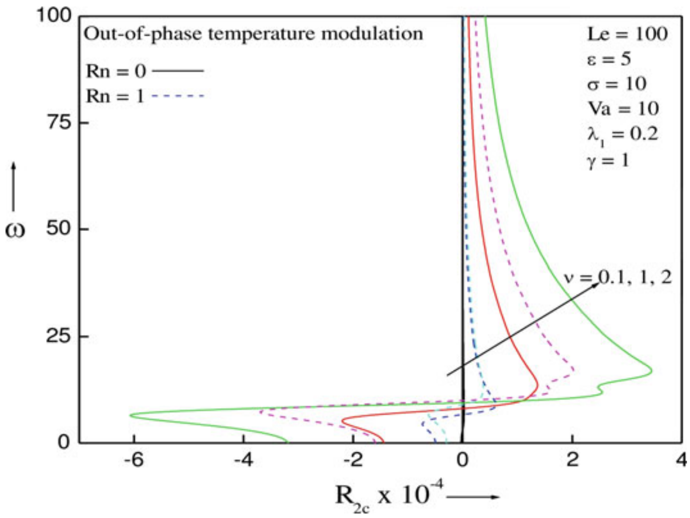

Fig. 14.15 Variation of R_{2c} with ω for different values of Rn and ν

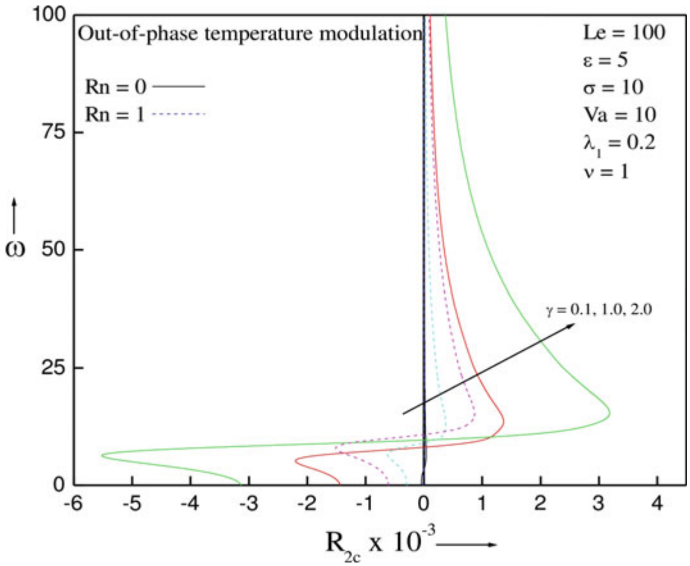

Fig. 14.16 Variation of R_{2c} with ω for different values of Rn and γ

From Figs. 14.1, 14.2, 14.3, 14.4, 14.5, 14.6, 14.7, 14.8, 14.9, 14.10, 14.11, 14.12, 14.13, 14.14, 14.15 and 14.16, one can observe that the peak values of for a regular fluid compared to a nanofluid for all the governing parameters. A nanofluid has a more stabilizing effect compared to a regular fluid.

Table 14.1 Nomenclature

c	Nanofluid specific heat at constant pressure	c_p	Specific heat of the nanoparticle material
$(\rho c)_m$	Effective heat capacity of the porous medium	d_p	Nanoparticle diameter
g	Gravitational acceleration	D_B	Brownian diffusion coefficient $\frac{m^2}{s}$
h_p	Specific enthalpy of the nanoparticle Specific enthalpy of the nanoparticle materialmaterial	H	Dimensional layer depth (m)
j_p	Diffusion mass flux for the nanoparticles	$j_{p,T}$	Thermophoretic diffusion
k	Thermal conductivity of the nanofluid	k_B	Boltzman constant
k_m	Effective thermal conductivity of the porous medium	k_p	Thermal conductivity of the particle material
Le	Lewis parameter	N_A	Modified diffusivity ratio
N_B	Modified particle-density increment	p^*	Pressure
p	Dimensionless pressure, $\frac{p^* K}{\mu \alpha_m}$	q	Energy flux relative to a frame moving with the nanofluid velocity
R	Thermal Rayleigh–Darcy number	Rn	Concentration Rayleigh number
t^*	time	t	Dimensionless time, $t^* \alpha_m / \sigma H^2$
T^*	Nanofluid temperature	T	Dimensionless temperature, $\frac{T^* - T_c^*}{T_h^* - T_c^*}$
T_c^*	Temperature at the upper wall	T_h^*	Temperature at the lower wall
T_R	Reference temperature	(u, v, w)	Dimensionless Darcy velocity components $\frac{(u^*, v^*, w^*)H}{\alpha_m}$
v	Nanofluid velocity	v_D	Darcy velocity εv
v_D^*	Dimensionless Darcy velocity (u^*, v^*, w^*)	γ_a	Non dimensional acceleration coefficient
Va	Vadász number	(x, y, z)	Dimensionless Cartesian coordinate
$\frac{(x^*, y^*, z^*)}{H}$	Vertically upward coordinate	(x^*, y^*, z^*)	Cartesian coordinates
Greek symbols			
α_m	Thermal diffusivity of the porous medium $\frac{k_m}{(\rho c)_f}$	$\tilde{\beta}$	Proportionality factor
γ	Conductivity variation parameter	λ_1	Relaxation parameter
ε	Porosity of the medium	ε_t	Amplitude of the modulation
μ	Viscosity of the fluid	ν	Viscosity variation parameter
ρ	Fluid density	ρ_p	Nanoparticle mass density
σ	Parameter	ϕ^*	Nanoparticle volume fraction

(continued)

Table 14.1 (continued)

ϕ	Relative nanoparticle volume fraction, $\frac{\phi^*-\phi_c^*}{\phi_h^*-\phi_c^*}$	Ω	Dimensional frequency
ω	Dimensionless frequency $\left(=\frac{\Omega H^2}{K}\right)$		
ψ	Phase angles		
$\psi=0$	Symmetric modulation	$\psi=\pi$	Antisymmetric modulation
$\psi=-i\infty$	Only lower wall temperature modulation		

14.7 Conclusion

The effect of thermal modulation on the onset of convection in a Maxwell fluid and nanofluid saturated porous layer was studied using a linear stability analysis and the following conclusions were drawn (Table 14.1):

1. The effect of all three types of modulations namely, symmetric, asymmetric, and only with lower wall temperature modulations is found to be destabilizing compared to the unmodulated system.
2. Low frequency symmetric modulation is destabilizing while high frequency symmetric modulation is always stabilizing for both regular and nanofluids.
3. Large values of the concentration Rayleigh number are found to stabilize the system for all types of modulations.
4. The viscosity and conductivity variation parameters produce more stability for the system.
5. The nanofluid is found to be more stabilizing compared to regular fluid in all three types of temperature modulations.

Acknowledgements One of the authors, J.C. Umavathi, is thankful for the financial support under the UGC-MRP F.43-66/2014 (SR) Project, and also to Prof. Maurizio Sasso, supervisor and Prof. Matteo Savino co-coordinator of the ERUSMUS MUNDUS "Featured eUrope and South/south-east Asia mobility Network FUSION" for their support to do Post-Doctoral Research.

References

1. Awad, F.G., Sibanda, P., Motsa, S.S.: On the linear stability analysis of a Maxwell fluid with double-diffusive convection. Appl. Math. Model. **34**, 3509–3517 (2010)
2. Braester, C., Vadász, P.: The effect of a weak heterogeneity of a porous medium on natural convection. J. Fluid Mech. **254**, 345–362 (1993)
3. Buongiorno, J.: Convective transport in nanofluids. ASME J. Heat Transf. **128**, 240–250 (2006)
4. Chen, H.S., Ding, Y.L., Tan, C.Q.: Rheological behavior of nanofluids. New. J. Phys. **9**, 1–25 (2007)

5. Choi, S.: Enhancing thermal conductivity of fluids with nanoparticles. In: Siginer, D.A., Wang, H.P. (eds.) Developments and Applications of Non-Newtonian Flows) 231/MD - 66, pp. 99–105. ASME, New York (1995)
6. Chung Liu, I.: Effect of modulation on onset of thermal convection of a second grade fluid layer. Int. J. Non-Linear Mech. **39**, 1647–1657 (2004)
7. Eastman, J.A., Choi, S.: LI, S., Thompson, L.J.: Anomalously increased effective thermal conductivities of ethylene-glycol-based nanofluids containing copper nanoparticles. Appl. Phys. Lett. **78**, 718–720 (2001)
8. El-Sayed, M.F.: Electro hydrodynamic instability of two superposed Walters B viscoelastic fluids in relative motion through porous medium. Arch. Appl. Mech. **71**, 717–732 (2001)
9. Finlayson, B.A.: The Method of Weighted Residuals and Variation Principles. Academic Press, New York (1972)
10. Gounot, J., Caltagirone, J.P.: Stabilite et convection naturelle au sein d'une couche poreuse non homogene. Int. J. Heat Mass Transf. **32**, 1131–1140 (1989)
11. Horton, W., Rogers, F.T.: Convection currents in a porous medium. J. Appl. Phys. **16**, 367–370 (1945)
12. Khayat, R.W.: Chaos and over stability in the thermal convection of viscoelastic fluids. J. Non-Newton. Fluid Mech. **53**, 227–255 (1994)
13. Leong, J.C., Lai, F.C.: Natural convection in rectangular layers porous cavities. J. Thermophys. Heat Transf. **18**, 457–463 (2004)
14. Malashetty, M.S., Begum, I.: Effect of thermal/gravity modulation on the onset of convection in a Maxwell fluid saturated porous layer. Transp. Porous Media **90**, 889–909 (2011)
15. Malashetty, M.S., Swamy, M., Heera, R.: The onset of convection in a binary viscoelastic fluid saturated porous layer. Z. Angew. Math. Mech. **89**, 356–369 (2009)
16. Masuda, H., Ebata, A., Teramae, K., Hishinuma, N.: Alteration of thermal conductivity and viscosity of liquid by dispersing ultra-fine particles. Netsu Bussei/Jpn. J. Thermophys. Prop. **7**, 227–233 (1993)
17. Maxwell, J.C.: On the dynamical theory of gases. Philos. Trans. R. Soc. Lond. Ser. A. **157**, 26–78 (1866)
18. McKibbin, R., O'Sullivan, M.J.: Heat transfer in a layered porous medium heated from below. J. Facil. Manag. **111**, 141–173 (1981)
19. Nield, D.A.: Convective heat transfer in porous media with columnar structures. Transp. Porous Media **2**, 177–185 (1987)
20. Nield, D.A.: General heterogeneity effects on the onset of convection in a porous medium. In: Vadász, P. (ed.) Emerging Topics in Heat and Mass Transfer in Porous Media, pp. 63–84. Springer, New York (2008)
21. Nield, D.A., Kuznetsov, A.V.: Thermal instability in a porous medium layer saturated by a nanofluid. Int. J. Heat Mass Transf. **52**, 5796–5801 (2009)
22. Nield, D.A., Kuznetsov, A.V.: The onset of convection in a layer of a porous medium saturated by a nanofluid: effects of conductivity and viscosity variation and cross diffusion. Transp. Porous Media **92**, 837–846 (2012)
23. Rees, D.A.S., Riley, D.S.: The three-dimensionality of finite-amplitude convection in a layered porous medium heated from below. J. Fluid Mech. **211**, 437–461 (1990)
24. Sekhar, G.N., Jayalatha, G.: Elastic effects on Rayleigh-Bénard convection in liquids with temperature-dependent viscosity. Int. J. Therm. Sci. **49**, 67–75 (2010)
25. Shivakumara, I.S., Lee, J., Malashetty, M.S., Sureshkumar, S.: Effect of thermal modulation on the onset of convection in Walters B viscoelastic fluid-saturated porous medium. Transp. Porous Media **87**, 291–307 (2011)
26. Siddheshwar, P.G., Srikrishna, C.V.: Unsteady nonlinear convection in a second-order fluid. Int. J. Nonlinear Mech. **37**, 321–330 (2002)
27. Siddheshwar, P.G., Sekhar, G.N., Jayalatha, G.: Effect of time-periodic vertical oscillations of the Rayleigh-Bénard system on nonlinear convection in viscoelastic liquids. J. Non-Newton. Fluid Mech. **165**, 1412–1418 (2010)

28. Simmons, C.T., Fenstemaker, T.R., Sharp, J.M.: Variable-density flow and solute transport in heterogeneous porous media: Approaches, resolutions and future challenges. J. Contam. Hydrol. **52**, 245–275 (2001)
29. Sokolov, M., Tanner, R.I.: Convective stability of a general viscoelastic fluid heated from below. Phys. Fluid **15**, 534–539 (1972)
30. Tan, W.C., Masouka, T.: Stability analysis of Maxwell fluid in a porous medium heated from below. Phys. Lett. A. **360**, 454–460 (2007)
31. Tiwari, R.K., Das, M.K.: Heat transfer augmentation in a two-sided lid-driven differentially heated square cavity utilizing nanofluids. Int. J. Heat Mass Transf. **50**, 2002–2018 (2007)
32. Tzou, D.Y.: Thermal instability of nanofluids in natural convection. Int. J. Heat Mass Transf. **51**, 2967–2979 (2008)
33. Umavathi, J.C.: Effect of thermal modulation on the onset of convection in a porous medium layer saturated by a nanofluid. Transp. Porous Media **98**, 59–79 (2013)
34. Vadász, P.: Heat transfer enhancement in nanofluids suspensions: possible mechanisms and explanations. Int. J. Heat Mass Transf. **48**, 2673–2683 (2005)
35. Vadász, P.: Heat conduction in nanofluid suspensions. ASME. J. Heat Transf. **128**, 465–477 (2006)
36. Wang, S., Tan, W.C.: Stability analysis of double-diffusive convection of Maxwell fluid in a porous medium heated from below. Phys. Lett. A. **372**, 3046–3050 (2008)